Special issue of the 2nd International Conference on Computational and Experimental Science and Engineering (ICCESEN 2015)

Frequency and Voltage-Dependent Dielectric Properties and AC Electrical Conductivity of (Au/Ti)/Al_2O_3/*n*-GaAs with Thin Al_2O_3 Interfacial Layer at Room Temperature

Ç.Ş. Güçlü[a], A.F. Özdemir[a,*], A. Kökce[a] and Ş. Altindal[b]
[a]Süleyman Demirel University, Physics Department, Isparta, Turkey
[b]Gazi University, Physics Department, Ankara, Turkey

An (Au/Ti)/Al_2O_3/n-GaAs structure with thin (30 Å) interfacial oxide layer (Al_2O_3), formed by atomic layer deposition technique is fabricated to investigate both frequency and applied bias voltage dependences of real and imaginary parts of dielectric constant (ε' and ε'') and electric modulus (M' and M''), loss tangent $\tan\delta$ and ac electrical conductivity σ_{AC} in a wide frequency range from 1000 Hz to 1 MHz at room temperature. The dielectric properties of the (Au/Ti)/Al_2O_3/n-GaAs metal-insulator-semiconductor structure are obtained using the forward and reverse bias capacitance-voltage (C-V) and conductance-voltage (G/ω-V) measurements in the applied bias voltage range from –4 V to +4 V, at room temperature. Experimental results show that the dielectric parameters were strongly frequency and voltage dependent. For each frequency the (C-V) plots show a peak and the change in frequency has effect on both the intensity and position of the peak. ε', ε'' and $\tan\delta$ decrease with increasing frequency, whereas σ_{AC} increases with increasing frequency at applied bias voltage. M' increases with the increasing frequency and reaches a maximum. M'' shows a peak and peak position shifts to higher frequency with increasing applied voltage. It can be concluded that the ε', ε'', $\tan\delta$, M', M'' and σ_{AC} values of the (Au/Ti)/Al_2O_3/n-GaAs structure are strongly dependent on both the frequency and applied bias voltage especially in the depletion and accumulation region. Also, the results can be deduced to imply that the interfacial polarization is easier at low frequencies, therefore contributing to the deviation of dielectric properties and AC electrical conductivity of (Au/Ti)/Al_2O_3/n-GaAs structure.

DOI: 10.12693/APhysPolA.130.325
PACS/topics: 73.30.+y

1. Introduction

The deposition of a thin interfacial layer between metal and semiconductor layers converts a metal-semiconductor (MS) structure into a metal-insulator-semiconductor (MIS) or metal-oxide-semiconductor (MOS) structure and thereby causes strong influence on characteristics of structure. To prevent the interface diffusion and reaction between metal and semiconductor, the formation of an interfacial insulator layer of SnO_2, Al_2O_3, TiO_2 or HfO_2 at MS interface, rather than the conventional SiO_2, has recently captured considerable attention of researchers in view of device applications. Especially, Al_2O_3 is important to evidence the effects of the native oxide defects such as oxygen vacancies and such defects as grain boundaries on the electrical and dielectric properties of MIS or MOS structures. Al_2O_3 is an attractive candidate for the high-k material. It has a wide band gap of about 6.6 eV and dielectric constant of 8.6 (for the amorphous oxide, typical for layers grown by atomic layer deposition (ALD)) [1–11].

ALD technique can be preferred to other techniques for the deposition of metallic gate oxide Al_2O_3 due to its unparalleled uniformity and precise thickness control technique. Owing to Al_2O_3, the structure behaves like a capacitor which stores electric charge by virtue of interfacial layer's dielectric property.

C-V and G/ω-V characteristics of MIS structure are controlled mainly by its interface properties. As is well-known, the C-V plot or admittance value, differ significantly from those expected for an ideal MIS diode, and thus the performance of the metal oxide/GaAs-based electronic devices is reduced [1–8]. Therefore, studies on interface properties are essential in the understanding of the electrical and dielectric properties of the MIS structures, and are especially of the technological importance for development of GaAs-based devices [8–10]. The interfacial parameters, such as the density of interface states N_{ss} and the thickness of interfacial layer, can influence both the electrical and dielectric behavior of these structures [11–16]. It is known that when localized states exist at the interface, the device behavior is different from the ideal case. Since the interface capacitance (excess capacitance) depends strongly on the frequency and applied voltage, the C-V and G/ω-V characteristics are affected.

The reason for choosing GaAs as the substrate is that GaAs has a direct energy band gap and it has attracted much attention due to its higher mobility, higher saturated electron velocity and higher breakdown field compared with traditional silicon. Generally, it is used in devices for high frequency and low power applications [11–15].

*corresponding author; e-mail: farukozdemir@sdu.edu.tr

In this study, we have prepared a MIS structure of (Au/Ti)/Al_2O_3/n-GaAs. The Al_2O_3 metal oxide layer on the n-GaAs substrate was formed by ALD method. The thin film thickness of the Al_2O_3 layer was about 3 nm. The frequency and voltage dependence of dielectric parameters were studied. By conducting at room temperature the frequency-dependent capacitance-voltage C-V-f and conductance-voltage G/ω-V-f measurements of (Au/Ti)/Al_2O_3/n-GaAs MIS structure we have examined the frequency-dependent changes in C-V, G/ω-V plots, in dielectric constant ε', dielectric loss ε'', loss tangent $\tan\delta$, ac electrical conductivity σ_{AC} and electric modulus M^*.

2. Experimental details

(Au/Ti)/Al_2O_3/n-GaAs MIS structure was fabricated using n-type single crystal GaAs wafer with (100) surface orientation, having thickness of 380 μm and carrier concentration N_D of 6.8×10^{15} cm^{-3} (given by the manufacturer). Before the MIS structure fabrication process, as a cleaning procedure, wafer was sonicated for five minutes in acetone and five minutes in isopropanol and then rinsed in DI water with resistivity of 18 MΩ cm for an extended time and dried under N_2 flow. After surface cleaning of n-GaAs, high purity (99.999%), ohmic contact was made by thermal evaporation of Au (2000 Å) metal on the back of the n-GaAs substrate, under vacuum of about 10^{-6} Torr. Low ohmic contact to n-GaAs was obtained by annealing at 385 °C for three minutes under dry nitrogen flow. The ALD of Al_2O_3 thin film was carried out in Cambridge Nanotech Savannah 100 reactor. The Al_2O_3 deposition was performed at 250 °C using trimethylaluminium (TMA) (Al precursor), and water (oxygen precursor), for a total 30 cycles. On Al_2O_3 interfacial layer, formed by ALD method, an Au(90 nm)/Ti(10 nm) Schottky contact was made using thermal evaporation technique. Finally the Schottky contacts have been formed as dots with diameter of about 1.0 mm on the front surface of Al_2O_3/n type GaAs with a shadow mask. The forward and reverse bias $C(V,f)$ and $G/\omega(V,f)$ measurements were carried out in frequency and applied voltage ranges of 1 kHz–1 MHz and −4 to +4 V, respectively, at room temperature, using a HP 4192 A LF impedance analyzer (5 Hz–13 MHz) and the test signal of 50 mV_{rms}. It is well known that the morphology of thin interfacial layer of Al_2O_3 and its homogeneity are very important for the device performance of MS and MIS structure. Figure 1 shows the schematic model of the (Au/Ti)/Al_2O_3/n-GaAs MIS structure.

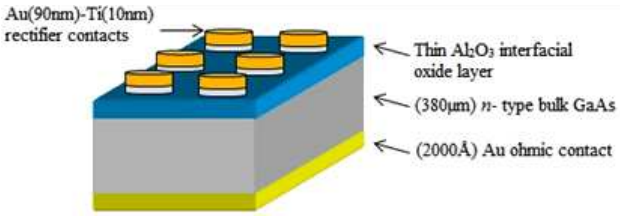

Fig. 1. Schematic model of the (Au/Ti)/Al_2O_3/n-GaAs MIS structure.

3. Results and discussion

3.1. Frequency dependence of C-V and G/ω-V characteristics

The capacitance-voltage C-V and conductance-voltage G/ω-V characteristics of Au/Ti/Al_2O_3/n-GaAs MIS structure were evaluated by capacitance C and conductance G measurements in the frequency range of 1 kHz–1 MHz by applying a small AC signal with amplitude of 50 mV from the external pulse generator, while the DC bias voltage was swept from −4 V to +4 V at room temperature. Results are given in Fig. 2a and b, respectively. The units of C and G are F and Ω^{-1} (or S), respectively. In order to compare the magnitude of C and G in the same scale, usually the value of G is divided by angular frequency.

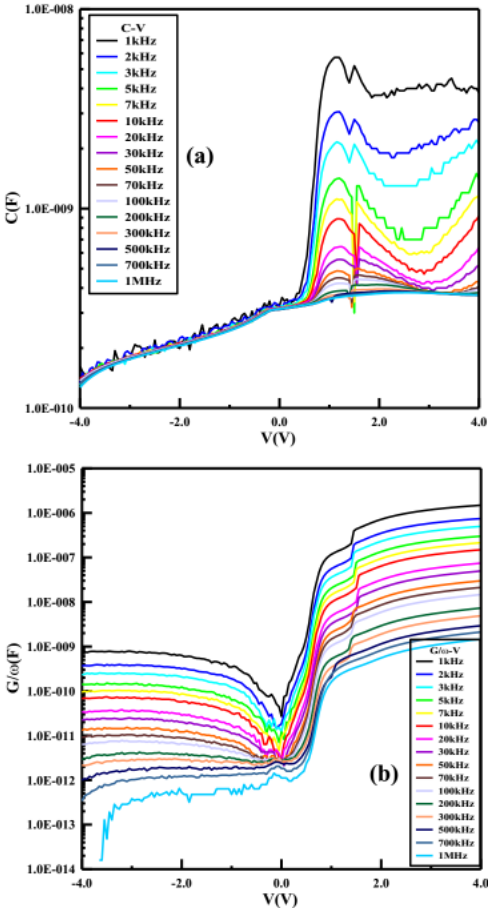

Fig. 2. The variation of the (a) C-V and (b) G/ω-V characteristics of the (Au/Ti)/Al_2O_3/n-GaAs MIS structure, measured for various frequencies.

As can be seen from Fig. 2a and b, both curves have three distinct regimes of inversion, depletion and accumulation. The value of C decreases with increasing

frequency and gives a broad peak for each frequency at accumulation region due to the effect of R_s (series resistance) and interfacial oxide layer. While the value of C decreases with applied bias voltage, G/ω increases in the accumulation region. At low frequencies, the high value of C and G/ω can be attributed to the excess capacitance C and conductance G, resulting from the density of interface states N_{ss} at Al_2O_3/n-GaAs interface. This indicates that at low frequencies (the value of period is higher than the time constant of the charge at traps), the N_{ss} can easily follow the AC signal and consequently contributes evidently to the diode capacitance and conductance [16–18]. At the sufficiently high frequencies, in contrast to the low frequency, ($f \geq 1$ MHz), the N_{ss} almost cannot follow the AC signal and do not contribute to the measured capacitance and conductance. In other words, at high frequencies, the carrier life time τ is much larger than period ($T = (2\pi f)^{-1}$) and so the charges at interface traps cannot follow the AC signal in contrast to the case of low frequencies.

In this study, the dielectric properties such as dielectric constant ε', dielectric loss ε'', loss tangent $\tan\delta$, the real and imaginary parts of electric modulus M' and M'' and AC electrical conductivity σ_{AC} of $(Au/Ti)/Al_2O_3/n$-GaAs structure were investigated using the dielectric spectroscopy [6–16] which includes C-V-f and G/ω-V-f measurements in the wide frequency range of 1 kHz to 1 MHz.

3.2. Frequency dependence of dielectric properties

The dielectric properties of MIS structure play an important in electronic device applications. For this reason, the detailed investigation of dielectric parameters, like AC electrical conductivity and electric modulus, is very important for determination of the device characteristics. The frequency and applied bias voltage dependence of real and imaginary parts (ε', ε'') of complex dielectric constant ε^* and loss tangent $\tan\delta$ of $(Au/Ti)/Al_2O_3/n$-GaAs structure were obtained from the C and G data in the frequency range of 1 kHz–1 MHz and voltage range of -4 V to $+4$ V, at room temperature.

Complex permittivity which is an important parameter in uncovering the electrical and dielectric properties of a structure, is described as [17, 19]

$$\varepsilon^* = \varepsilon' - i\varepsilon'', \tag{1}$$

where i is the imaginary root of $\sqrt{-1}$. Given the admittance measurements, this can be written as

$$\varepsilon^* = \frac{Y^*}{i\omega C_0} = \frac{C}{C_0} - i\frac{G}{\omega C_0}, \tag{2}$$

where Y^*, C and G are the measured admittance, capacitance and conductance values of the dielectric material, respectively, and ω is the angular frequency. The dielectric constant ε' can be calculated from the measured capacitance C_{ma} values in the strong accumulation region at different frequencies using the following equation [20, 21]:

$$\varepsilon' = \frac{C_{ma}}{C_0} = \frac{C_{ma} d_{ox}}{\varepsilon_0 A}, \tag{3}$$

where $C_0 = \varepsilon_0 A/d_{ox}$ is capacitance of an empty capacitor, A is the rectifier contact area (in this study 0.01 cm^2) and ε_0 is the electric permittivity of free space $\varepsilon_0 = 8.85 \times 10^{-14}$ F cm^{-1}. In the strong accumulation region, the maximum capacitance of the structure corresponds to the capacitance of the insulator oxide layer $C_m = C_i = \varepsilon'\varepsilon_0 A/d_{ox}$. Dielectric loss ε'' can be calculated from the measured conductance G_{ma} values in the strong accumulation region at different frequencies using the following equation:

$$\varepsilon'' = \frac{G_{ma}}{\omega C_0} = \frac{G_{ma} d_{ox}}{\varepsilon_0 \omega A}. \tag{4}$$

The loss tangent $\tan\delta$ is defined by the relation [17, 21]

$$\tan\delta = \frac{\varepsilon''}{\varepsilon'}. \tag{5}$$

The frequency dependence of ε', ε'' and $\tan\delta$ profiles as functions of bias voltage were obtained from Eqs. (3), (4) and (5), respectively. They are given in Fig. 3a–c, respectively.

As shown in Fig. 3a, the value of ε' increases with increasing applied bias voltage for each frequency both in depletion and accumulation regions, however curves start bending in accumulation region due to effect of series resistance, in the range between +1 V and +1.5 V of applied bias voltage. The value of ε'', exhibits the opposite behavior in comparison with ε' (Fig. 3b). While the value of ε' increases/decreases with increasing applied bias voltage, the value of ε'' decreases/increases like C and G/ω (Fig. 2a and b). As shown in Fig. 3a, ε' exhibits much the same value in the inversion region, for each frequency. Such behavior of C and G/ω or ε' and ε'' is known as inductive behavior, due to the effect of R_s and surface states [22, 23]. The $\tan\delta$ versus V plot for each frequency also exhibits U-shape behavior like the ε'' versus V plot, due to inductive behavior of the structure.

The profiles of ε', ε'' and $\tan\delta$ versus V are found to be similar to the plots of C-V in Fig. 2a and G/ω-V in Fig. 2b, due to the same reasons. This behavior can be attributed to the interfacial effect within the bulk of the sample, interfacial oxide layer, interfacial traps, surface polarization and electrode effect [11–15]. In the $\tan\delta$-V plot in Fig. 3c, the structure has a peak behavior both in inversion and depletion region, depending on ε' and ε'' values.

In addition, as can be seen in Fig. 3a and b, ε' and ε'' values decrease with increasing frequency. These results are quite compatible with those found in a different material [23]. The fact that ε' and ε'' values are greater at low frequencies could be attributed to the presence of a possible interface polarization mechanism, since interface states cannot follow the AC signal at high frequencies and do not contribute to the capacitance, due to the lack of any interface polarization mechanism [21]. In general, polarization mechanisms at low frequencies are affected by electronic, ionic, dipolar and interface or surface polarization distribution [24, 25]. The high values of ε'

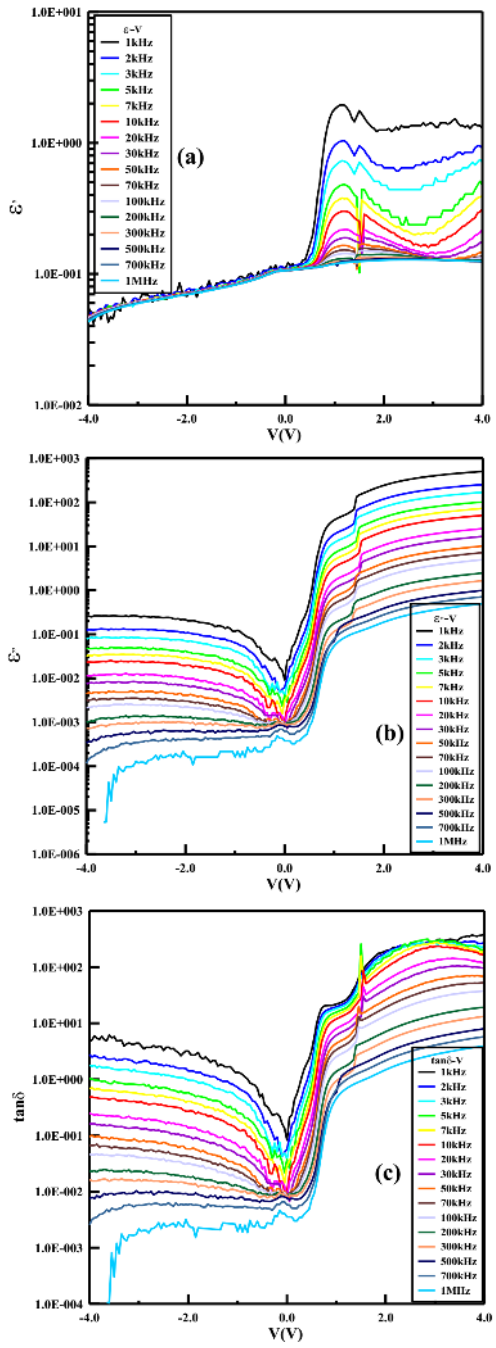

Fig. 3. The frequency dependence of the (a) ε' versus V, (b) ε'' versus V and (c) $\tan\delta$ versus V, between -4 V and $+4$ V, for (Au/Ti)/Al_2O_3/n-GaAs MIS structure, at room temperature.

and ε'' investigated at low frequencies may be attributed to interfacial Maxwell-Wagner polarization [26] and space charge polarization [27].

There are many studies on the complex electric modulus M^* formalism with regard to the analysis of dielectric or insulator materials [27, 28]. The complex impedance Z^* or the complex permittivity $\varepsilon^* = 1/M^*$ data are transformed into the M^* formalism using the following relation [11, 26–28].

$$M^* = i\omega C_0 Z^*, \tag{6a}$$

$$M^* = \frac{1}{\varepsilon^*} = M' + iM'' = \frac{\varepsilon'}{\varepsilon'^2 + \varepsilon''^2} + i\frac{\varepsilon''}{\varepsilon'^2 + \varepsilon''^2}, \tag{6b}$$

where i is the imaginary root of $\sqrt{-1}$, ω is angular frequency. The real M' and imaginary M'' parts of complex electric modulus M^* of the (Au/Ti)/Al_2O_3/n-GaAs MIS structure were obtained using ε' and ε'' values (Eqs. (6a) and (6b)) and are given in Fig. 4a and b, respectively, to see the effect of applied bias voltage.

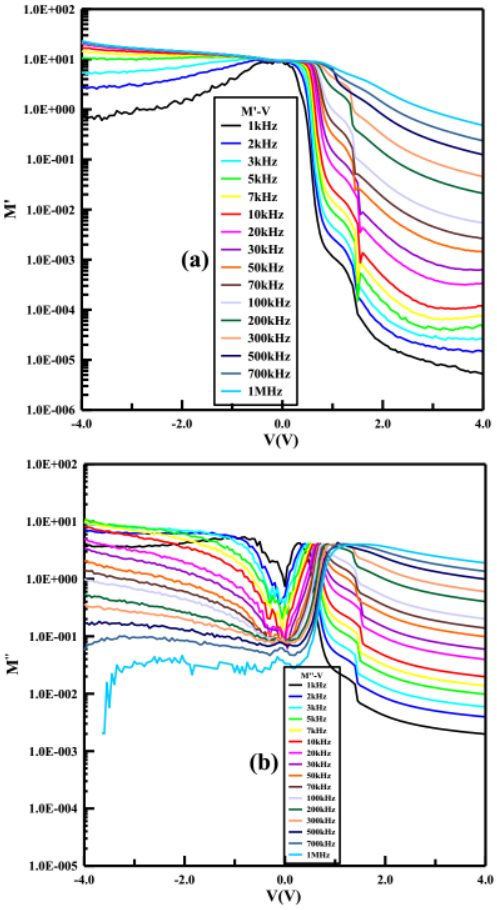

Fig. 4. The frequency dependence of the (a) M' versus V and (b) M'' versus V of (Au/Ti)/Al_2O_3/n-GaAs MIS structure, measured between -4 V and $+4$ V, at room temperature.

Figure 4a and b shows the frequency-dependent changes in the real M' and imaginary M'' components of the electric modulus of the MIS structure at applied bias voltage. It is clear that both the value of M' and M'' have an evident frequency and voltage dispersion, especially at inversion and accumulation regions. M'-V and M''-V plots, given in Fig. 4a and b, respectively, are also obtained by using Eqs. (6a) and (6b) for various frequencies. M' and M'' are strong functions of applied bias voltages, especially in the depletion region and M' and M'' values give a peak and magnitude of peak increase with the decreasing frequency, due to the contribution

to the interface trap charges. Such behavior of M'-V and M''-V plots can be explained by the dielectric relaxation mechanisms sensitive to frequency rather than to applied bias voltage. The peak in the inversion and depletion region can be attributed to the particular density distribution of interface traps located at Al_2O_3/n-GaAs interface and their relaxation times [18, 24]. On the other hand, while the M' reaches a minimum value, M'' reaches maximum value, which is corresponding to $M_\infty = 1/\varepsilon_\infty$, due to inductive behaviour of the MIS structure and the relaxation process.

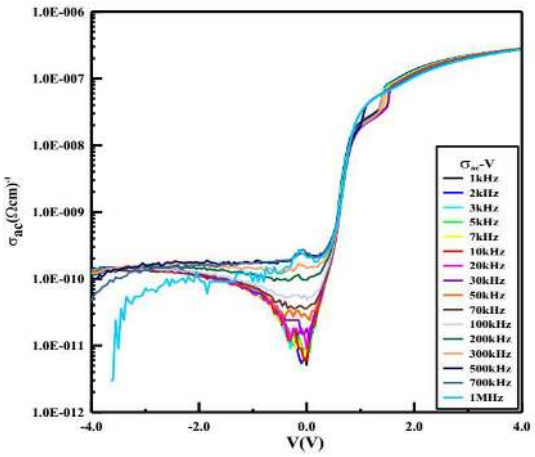

Fig. 5. The frequency dependence of the (a) σ_{AC} versus V of (Au/Ti)/Al_2O_3/n-GaAs MIS structure, measured between -4 V and $+4$ V, at room temperature.

The voltage dependent AC electrical conductivity σ_{AC} of the (Au/Ti)/Al_2O_3/n-GaAs MIS structure is given by the Eq. (7) [28], and is shown in Fig. 5, for various applied bias voltages, for room temperature.

$$\sigma_{AC} = \omega C \tan\delta \frac{d_{ox}}{A} = \varepsilon'' \omega \varepsilon_0. \tag{7}$$

It is clear that in Fig. 5, the value of AC electrical conductivity in the reverse bias region generally decreases with increasing applied bias voltage almost linearly for each frequency, but in the accumulation region increase with the increasing applied bias voltage is almost linear. Besides, the change in σ_{AC} in the depletion region (-1 V–0 V) it decreases almost exponentially with increasing voltage for each frequency. In the addition, the opposite behaviour in inverse and accumulation regions of ε' and ε'' can be explained in the respect of inductive behavior of the MIS structure. The increase of AC electrical conductivity with increasing frequency leads to an increase in the eddy current, which in turn increases in the energy loss $\tan\delta$.

4. Conclusions

Dielectric properties and electrical conductivity of (Au/Ti)/Al_2O_3/n-GaAs MIS structure have been studied in the frequency range of 1 kHz–1 MHz and voltage range of -4 V to $+4$ V, at room temperature. In this work, Al_2O_3 interfacial oxide layer (with a thickness of 30 Å) was used as a high dielectric interfacial insulator layer between metal and semiconductor to improve the performance of MIS structure. Experimental results indicate that the main electrical and dielectrical parameters of (Au/Ti)/Al_2O_3/n-GaAs MIS structure were found to be strong functions of frequency and applied bias voltage, especially, in the depletion and accumulation regions, due mainly to the interfacial polarization and interface traps. From the analysis of the experimental results, it was concluded that ε', ε'' and $\tan\delta$ exhibit a steep decrease with increasing frequencies for each forward bias voltage, whereas σ_{AC} increases with the increasing frequency. The dispersion in ε' and ε'' at low frequencies is considerably high, which can be attributed to the Maxwell-Wagner and space charge polarization. The large values of ε' may be due to the interfacial effects within the material, Al_2O_3 interfacial layer and electron effect. On the other hand, the large values of ε'' are also due to the motion of free charge carriers within the material. Good dielectric properties of (Au/Ti)/Al_2O_3/n-GaAs MIS structure suggest their usage in possible applications such as high frequency transformers and high dielectric capacitors.

In addition, M' and M'' are strong functions of applied bias voltages, especially in depletion region and M' and M'' values give a peak and magnitude of peak increases with decreasing frequency due to the contribution to the interface trap charges. Such behavior of M'-V and M''-V plots can be explained by the dielectric relaxation mechanisms sensitive to frequency rather than applied bias voltage.

Acknowledgments

This work is financially supported by The Management Unit of Scientific Research Projects of Süleyman Demirel University (SDUBAP) under 4429-D2-15.

References

[1] A. Türüt, A. Karabulut, K. Ejderha, N. Bıyıklı, *Mater. Res. Express* **2**, 046301 (2015).

[2] A. Türüt, A. Karabulut, K. Ejderha, N. Bıyıklı, *Mater. Sci. Semicond. Processing* **39**, 400 (2015).

[3] D.E. Yıldız, M. Yıldırım, M. Gökçen, *J. Vac. Sci. Tech. A* **32**, 031509 (2014).

[4] R.D. Long, P. McIntyre, *Materials* **5**, 1297 (2012).

[5] H. Saghrouni, S. Jomni, W. Belgacem, N. Elghoul, L. Beji, *Mater. Sci. Semicond. Process* **29**, 307 (2015).

[6] C.P. Colinge, C.A. Colinge, *Physics of Semiconductor Devices*, Kluwer, Dordrecht 2002.

[7] S. Dimitrijev, *Principles of Semiconductor Devices*, Oxford University Press, Oxford 2012.

[8] A.F. Özdemir, S.G. Aydın, D.A. Aldemir, S.S. Gürsoy, *Synth. Met.* **161**, 692 (2011).

[9] D.A. Neamen, *Semiconductor Physics and Devices*, Irwin, Boston 1992.

[10] E.H. Rhoderick, R.H. Williams, *Metal-Semiconductor Contacts*, 2nd ed., Clarendon, Oxford 1988.

[11] A. Kaya, S. Alialy, S. Demirezen, M. Balbaşı, S.A. Yerişkin, A. Aytimur, *Ceram. Int.* **42**, 3322 (2016).

[12] E.E. Tanrıkulu, D.E. Yıldız, A. Günen, Ş. Altındal, *Phys. Scripta* **90**, 095801 (2015).

[13] İ. Yücedağ, A. Kaya, Ş. Altındal, İ. Uslu, *Chin. Phys. B* **23**, 047304 (2014).

[14] P.B. Macedo, C.T. Moyniham, R. Bose, *Phys. Chem. Glass* **13**, 171 (1972).

[15] S.M. Sze, *Physics of Semiconductor Devices*, 2nd ed., Willey & Sons, New York 1981.

[16] E.H. Nicollian, J.R. Brews, *Metal Oxide Semiconductor (MOS) Physics and Technology*, 2nd ed., Wiley, New York 1982.

[17] C.P. Symth, *Dielectric Behaviour and Structure*, 2nd ed., McGraw-Hill, New York 1955.

[18] V.V. Daniel, *Dielectric Relaxation*, 2nd ed., Academic, London 1967.

[19] M. Popescu, I. Bunget, *Physics of Solid Dielectrics*, 2nd ed., Elsevier, Amsterdam 1984.

[20] A. Chelkowski, *Dielectric Physics*, 2nd ed., Elsevier, Amsterdam 1980.

[21] B. Tataroğlu, Ş. Altındal, A. Tataroğlu, *Microelectron. Eng.* **83**, 2021 (2006).

[22] A.A. Sattar, S.A. Rahman, *Phys. Status Solidi A* **200**, 415 (2003).

[23] C. Fanggao, G.A. Saunders, E.F. Lampson, R.N. Hampton, G. Carini, G.D. Marco, M. Lanza, *J. Polym. Sci. Pol. Phys.***34**, 425, (1996).

[24] B. Barış, *Physica B* **438**, 53 (2014).

[25] M. Le-Huu, H. Schmitt, S. Noll, M. Grieb, F.F. Schrey, A.J. Bauer, L. Frey, H. Ryssell, *Microelectron. Reliab.* **51**, 1346 (2011).

[26] S. Alialy, Ş. Altındal, E.E. Tanrıkulu, D.E. Yıldız, *J. Appl. Phys.* **116**, 083709 (2014).

[27] Ö. Vural, Y. Şafak, A. Türüt, Ş. Altındal, *J. Alloys Compd.* **513**, 107 (2012).

[28] D.E. Yıldız, Ş. Altındal,Z. Tekeli, M. Özer, *Mater. Sci. Semicond. Process* **13**, 34 (2010).